

## Correspondence

The case of data fusion of sensors dissimilar in their measurement/tracking errors is considered. It is shown that the fused track performance is similar whether the sensor data is fused at the track level or at the measurement level. The case of a cluster of targets, resolved by one sensor but not the other, is also considered. Under certain conditions the fused track may perform worse than the worst of the sensors. A remedy to this problem through modifications of the association algorithm is presented.

### I. INTRODUCTION

The problem of multitarget tracking by multiple sensors received considerable attention in recent years (for example [1, 2]). The pay-off from combining data from a variety of sensors to extend the overall system performance envelope is obvious. The sensor fusion may be carried out by either combining sensor tracks or sensor observations.

Track fusion was studied by Singer and Kanyuck [3], who assumed independent process noise at each sensor. A practical implementation is shown in [4]. Bar-Shalom refined the track fusion equations by accounting for the common process noise observed at the sensors [5]. An alternative approach is to fuse sensor observations rather than tracks [7]. The track fusion approach is very attractive to the system designer. It is simpler to implement, in particular with existing systems, and being decentralized it is more robust with respect to sensor failures. A comparison of the fusion based on tracks and measurements is presented in [6].

Of particular interest in sensor fusion is the case involving two sensors dissimilar in their resolving capabilities. For example passive infrared (IR) seekers have typically higher angular resolution than radars, but do not provide direct range measurements. Thus sensor fusion may result in a performance envelope which expresses the best performance from each sensor. The situation is not as straightforward in the case of a cluster of targets. The cluster of targets may be resolved by one sensor (IR) but not by the other (radar). The special problems arising in such cases are reviewed here and ways to deal with them are suggested.

Manuscript received August 22, 1991, revised February 8, 1992.

IEEE Log No. T-AES/29/1/02258.

0018-9251/93/\$3.00 © 1993 IEEE

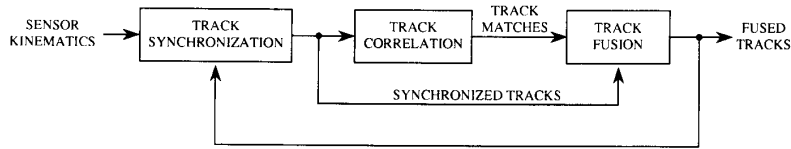


Fig. 1. Multisensor tracker.

## II. MULTISENSOR TRACKER

The target motion is modeled as

$$\mathbf{x}_{k+1} = \Phi \mathbf{x}_k + \Gamma \mathbf{v}_k \quad (1)$$

where  $\mathbf{x}_k$  is the state vector at time  $k$ ,  $\Phi$  is the state transition matrix,  $\mathbf{v}_k$  is the process noise and  $\Gamma$  is the process noise transition matrix. The state vector is assumed to consist of position and rate kinematic variables. The state and process noise transition matrices are given by

$$\Phi = \begin{pmatrix} 1 & \Delta \\ 0 & 1 \end{pmatrix} \quad (2)$$

and

$$\Gamma = \begin{pmatrix} \frac{1}{2}\Delta^2 \\ \Delta \end{pmatrix} \quad (3)$$

respectively. The time between observations is  $\Delta$ . The process noise  $\mathbf{v}_k$  has acceleration units and is described by a Gaussian random process with  $E[\mathbf{v}_k] = 0$  and  $E[\mathbf{v}_k \mathbf{v}_l] = \sigma_v^2 \delta_{kl}$ .

The measurement equation of the  $i$  and  $j$  sensors is given by

$$z_k^m = H \mathbf{x}_k^m + w_k^m \quad (4)$$

where  $m = i, j$ . The variable  $w_k^m$  is the observation noise with  $E[w_k] = 0$  and  $E[w_k w_l] = \sigma_w^2 \delta_{kl}$ . The sensor observation matrix is given by  $H = [1 \ 0]$ . Tracks are filtered and predicted at the sensor level using conventional tracking methods such as the Kalman or  $\alpha - \beta$  filters. The sensor level tracks are subsequently fused by the multisensor tracker.

The multisensor tracker consists of three main functions: 1) fusion, 2) synchronization, and 3) correlation. A schematic diagram of a multisensor tracker is shown in Fig. 1. The multisensor tracker fuses either the filtered state vectors  $\hat{\mathbf{x}}_{k/k}^i, \hat{\mathbf{x}}_{k/k}^j$  of the sensors or the measurements  $z_k^i, z_k^j$  of the sensors. Following Bar-Shalom we have for the state vector fusion [6],

$$\hat{\mathbf{x}}_{k/k}^f = \hat{\mathbf{x}}_{k/k}^i + \mathbf{C}_k^{ij} [\hat{\mathbf{x}}_{k/k}^j - \hat{\mathbf{x}}_{k/k}^i] \quad (5)$$

$$\mathbf{C}_k^{ij} = [\hat{\mathbf{P}}_{k/k}^i - \hat{\mathbf{P}}_{k/k}^{ij}] [\hat{\mathbf{P}}_{k/k}^i + \hat{\mathbf{P}}_{k/k}^j - \hat{\mathbf{P}}_{k/k}^{ij} - \hat{\mathbf{P}}_{k/k}^{ii}]^{-1} \quad (6)$$

$$\hat{\mathbf{P}}_{k/k}^f = \hat{\mathbf{P}}_{k/k}^i - \mathbf{C}_k^{ij} [\hat{\mathbf{P}}_{k/k}^i - \hat{\mathbf{P}}_{k/k}^{ij}]' \quad (7)$$

$$\hat{\mathbf{P}}_{k/k}^{ij} = [\mathbf{I} - \mathbf{C}_k^{ij} \mathbf{H}] \hat{\mathbf{P}}_{k/k-1}^{ij} [\mathbf{I} - \mathbf{C}_k^{ij} \mathbf{H}]' \quad (8)$$

where an apostrophe denotes matrix transposition,  $\hat{\mathbf{x}}_{k/k}^f$  is the fused state vector estimate,  $\mathbf{C}_k^{ij}$  is the fusion gain, and  $\hat{\mathbf{P}}_{k/k}^f, \hat{\mathbf{P}}_{k/k}^i, \hat{\mathbf{P}}_{k/k}^j$  are the filtered covariance estimates of the respective state vectors.  $\hat{\mathbf{P}}_{k/k}^{ij}$  is the cross covariance matrix between  $\hat{\mathbf{x}}_{k/k}^i$  and  $\hat{\mathbf{x}}_{k/k}^j$  and  $\mathbf{C}_k^m, m = i, j$ , are the sensor tracker gains.

In the measurement fusion approach the multisensor tracker fuses the sensor observations directly and uses a Kalman filter to estimate the fused state vector. The equations describing this process are:

$$\hat{\mathbf{x}}_{k/k}^f = \hat{\mathbf{x}}_{k/k-1}^f + \mathbf{W}_k^f [z_k - \mathbf{G} \hat{\mathbf{x}}_{k/k-1}^f] \quad (9)$$

$$\mathbf{W}_k^f = \hat{\mathbf{P}}_{k/k-1}^f \mathbf{G}' [\mathbf{G} \hat{\mathbf{P}}_{k/k-1}^f \mathbf{G}' + \mathbf{R}]^{-1} \quad (10)$$

$$\hat{\mathbf{P}}_{k/k}^f = [\mathbf{I} - \mathbf{W}_k^f \mathbf{G}] \hat{\mathbf{P}}_{k/k-1}^f \quad (11)$$

where  $\mathbf{W}_k^f$  is a  $2 \times 2$  Kalman weight matrix, and  $\mathbf{G}$  and  $\mathbf{R}$  are the combined observation and combined measurement noise matrices, respectively, given by

$$\mathbf{G} = \begin{pmatrix} 1 & 0 \\ 1 & 0 \end{pmatrix} \quad (12)$$

$$\mathbf{R} = \begin{pmatrix} \sigma_{w_i}^2 & 0 \\ 0 & \sigma_{w_j}^2 \end{pmatrix} \quad (13)$$

$\sigma_{w_i}^2, \sigma_{w_j}^2$  are the respective sensor measurement errors.

The data needs to be time synchronized to be processed by the correlation algorithm. The synchronization function in effect implements the prediction equations of the Kalman filter. In both track or measurement fusion approaches, the sensor data and covariance are predicted from time  $l$  to time  $k$  using the relations

$$\hat{\mathbf{x}}_{k/l}^m = \Phi_{k-l} \hat{\mathbf{x}}_{l/l}^m \quad (14)$$

$$\hat{\mathbf{P}}_{k/k}^m = \Phi_{k-l} \mathbf{P}_{k/k-1}^m \Phi_{k-l}' + \mathbf{Q}_{k-l} \quad (15)$$

$\Phi_{k-l}$  is the state transition matrix from time  $k$  to time  $l$ ,

$$\Phi = \begin{pmatrix} 1 & (k-l)\Delta \\ 0 & 1 \end{pmatrix} \quad (16)$$

$\mathbf{P}^m$  is the fixed sensor track covariance matrix, and  $\mathbf{Q}_{k-l} = \Gamma_{k-l} \Gamma_{k-l}'$ , with  $\Gamma_{k-l} = [\frac{1}{2}(k-l)^2 \Delta^2 \ (k-l)\Delta]'$ .

The association function is a decision algorithm that performs the sensor-to-sensor correlation. A common approach is to use the generalized likelihood

test statistic [8]

$$d_{ij} = \frac{1}{M} (z_k^i - z_k^j)' (S_{k/k}^i + S_{k/k}^j)^{-1} (z_k^i - z_k^j) \quad (17)$$

where  $M$  is the problem dimensionality (number of kinematic variables). The elements of the vectors  $z_k^m$  are sensor tracks/observations, and  $S_{k/k}^m$  are the covariance matrices of the tracks/observations of the sensors.

### III. EFFECT OF SENSOR MEASUREMENT/TRACKING ACCURACY

#### A. Single Target Case

The tracking error of fused sensors is dependent on the individual sensor accuracy. Previous work by Roecker and McGillem has shown that fusing sensor measurements provides the optimal solution while track fusion is suboptimal [6]. However the differences between the two approaches are smaller as the two sensors become increasingly dissimilar in their accuracies. This can be seen from the fusion equations. For  $P^i \ll P^j$ ,  $C^{ij} \approx 0$ , and  $x^f \approx x^i$ , the fused track error  $P^f \approx P^i$ .

A steady-state analysis of the track error was carried out to demonstrate the effect of sensor accuracy on the fused track error. Fig. 2 shows the differences in the elements of the error covariance matrix of the fused track for the two approaches, as a function of the measurement accuracy ratio of the two sensors. The normalized error difference  $r_{m,n}$  is defined

$$r_{m,n} = \frac{|P_{\infty M}^f(m,n) - P_{\infty T}^f(m,n)|}{P_{\infty M}^f(m,n)} \quad (18)$$

where  $P_{\infty M}^f, P_{\infty T}^f$  are the fused track steady state covariance for the measurements and track fusion, respectively.

For example, consider two sensors with an azimuth measurement accuracy ratio of 1 : 10,  $\sigma_w^i = 0.2^\circ$  and  $\sigma_w^j = 2.0^\circ$ . Assume both sensors are delivering their measurements synchronously at  $\Delta = 1$  s intervals. The process noise is assumed common to both sensors and it corresponds to an angular acceleration of  $\sigma_v = 0.0115^\circ/s^2$  (1g maneuver at 27 nmi). Fig. 3(a) shows the simulated track resultant from the measurements fusion of the sensor. The fused track steady-state error covariance and gain matrices were found in closed-form using relations developed in [10] and were confirmed via a simulated Kalman filter:

$$P_{\infty M}^f = \begin{bmatrix} 0.0114 & 0.0019 \\ 0.0019 & 0.0007 \end{bmatrix} \quad W_{\infty}^f = \begin{bmatrix} 0.2851 & 0.0029 \\ 0.0483 & 0.0005 \end{bmatrix}$$

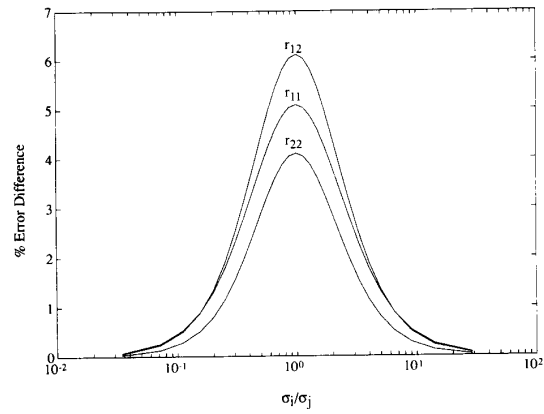


Fig. 2. Difference between measurement and track fusion steady-state errors.

Fig. 3(b) shows the simulated track resultant from the sensor level track fusion. Steady-state error covariance and gain matrices for the sensor level tracks were found in closed-form using optimal  $\alpha - \beta$  tracker techniques defined by Kalata in [11] and confirmed via simulated Kalman filters. The optimal  $\alpha - \beta$  tracker [11] matches the results of the steady-state Kalman filter

$$\begin{aligned} \alpha^i &= 0.2873 & \alpha^j &= 0.1017 \\ \beta^i &= 0.0485 & \beta^j &= 0.0055 \\ P_{\infty}^i &= \begin{bmatrix} 0.0115 & 0.0019 \\ 0.0019 & 0.0007 \end{bmatrix} & P_{\infty}^j &= \begin{bmatrix} 0.4068 & 0.0218 \\ 0.0218 & 0.0024 \end{bmatrix} \\ C_{\infty}^i &= \begin{bmatrix} 0.2873 \\ 0.0485 \end{bmatrix} & C_{\infty}^j &= \begin{bmatrix} 0.1017 \\ 0.0055 \end{bmatrix} \end{aligned}$$

Track fusion performance was calculated in closed-form using the  $\alpha - \beta$  linear combiner in [10] and confirmed via simulation

$$P_{\infty T}^f = \begin{bmatrix} 0.0114 & 0.0019 \\ 0.0019 & 0.0007 \end{bmatrix}$$

The error covariance matrix is the same for both fusion methods. This is also shown graphically in Fig. 3(c).

#### B. Cluster Case

The case of a cluster of targets resolved by one sensor but not the other is often encountered in applications of sensor fusion. For example in the fusion of radar and IR tracks. This problem may be approached in a number of ways and those are analyzed in the following.

One approach to this problem is to use all available data to generate a single multisensor track. Targets within predefined gates are assigned to the cluster and contribute to the fusion. Applying the nearest neighbor correlation approach to this case (at each

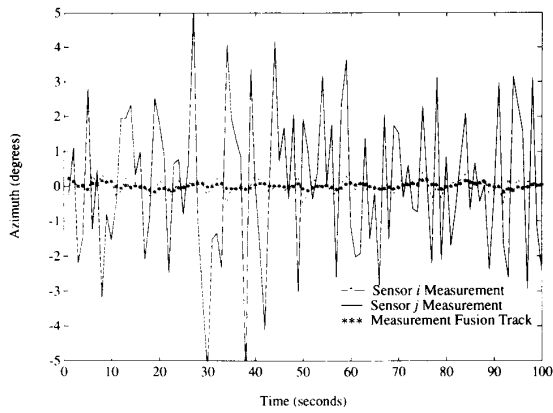


Fig. 3(a). Measurement fusion.

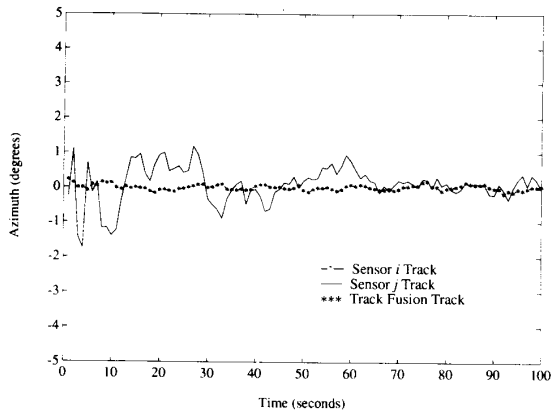


Fig. 3(b). Track fusion.

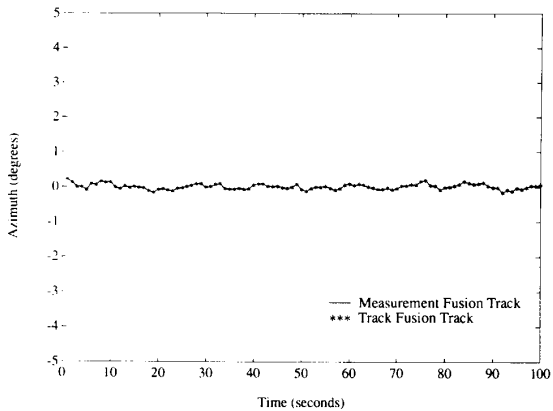


Fig. 3(c). Comparison between track fusion and measurement fusion.

frame selecting for fusion the two closest tracks) may lead to large errors. An example of this situation for angle tracking is shown in Fig. 4. The figure shows the high resolution tracks generated by sensor  $i$ , as well as the low resolution track of sensor  $j$ . The simulation considered angle tracking with measurement accuracy

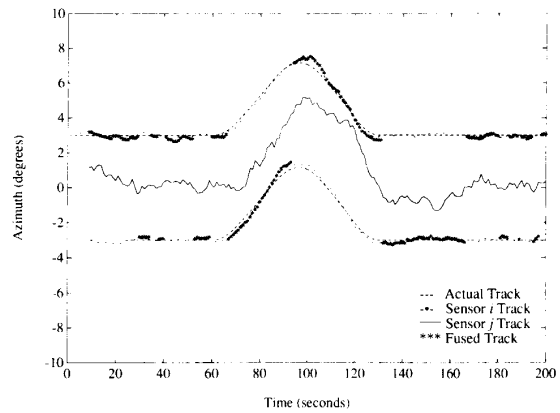


Fig. 4. Sensor fusion for cluster of targets. Single fused track, nearest neighbor correlation.

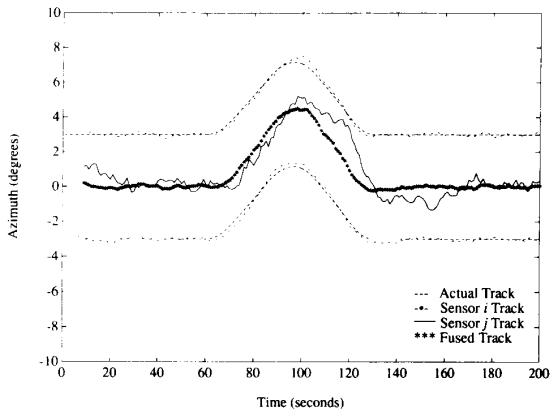


Fig. 5. Sensor fusion for cluster of targets. Single fused track, all tracks correlation.

of  $0.2^\circ$  for sensor  $i$ ,  $2^\circ$  for sensor  $j$  and resolution of  $6^\circ$  for sensor  $j$  (in radar systems, for example, resolution is a function of antenna beamwidth, while accuracy depends on the signal-to-noise ratio as well [9], thus the sensor resolution could be several times larger than the sensor track accuracy). For this case the data fusion results in a net increase in tracking error, and the performance of this multisensor track is worse than the worst of the sensor tracks.

Two ways are suggested to solve this problem. In the first solution, all sensor  $i$  tracks within a specified gate are correlated to the single sensor  $j$  track. The fused track is the centroid of all the correlated data. The simulation results with this solution incorporated is shown in Fig. 5. Note that the multisensor track follows now the centroid of the targets. The correlation gate size is calculated from the relation:

$$g_{ij} = \frac{1}{M} \mathbf{d}'_r (\hat{\mathbf{S}}_{k/k}^i + \hat{\mathbf{S}}_{k/k}^j)^{-1} \mathbf{d}_r \quad (19)$$

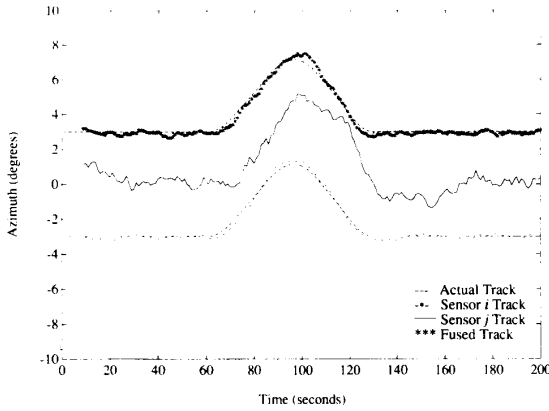


Fig. 6. Sensor fusion for cluster of targets. Single fused track, biased nearest neighbor correlation.

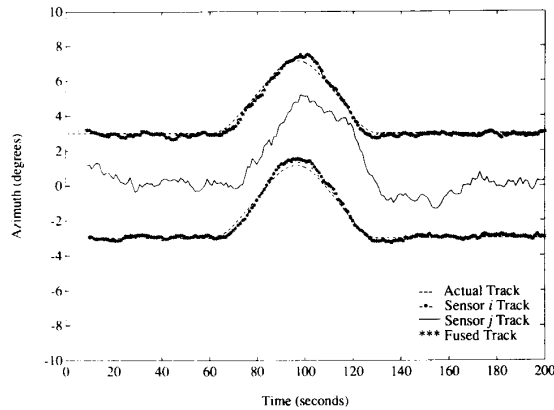


Fig. 7. Sensor fusion for cluster of targets. Multiple fused tracks, low resolution sensor imparts data to all tracks in cluster.

where  $\mathbf{d}_i$  is a vector whose elements are equal to the resolution for each track variable.

Another possible solution is to bias the normalized distance in (21) such that the correlation algorithm favors one target in the cluster. The simulation run using this approach is shown in Fig. 6. The normalized distance for the correlation algorithm was calculated from

$$d_{ij}^b = d_{ij} - b \quad (20)$$

where  $b$  was set equal to the normalized distance corresponding to half the resolution cell.

Another approach to the problem of fusing a single low resolution track to multiple high resolution tracks is to generate a track for each target in the cluster. The low resolution track will impart its information to all the targets in the cluster. For the particular example of fusion of radar and IR, it means that the same radar range data will be used to evolve all the multisensor tracks. The simulation run for this case is shown in Fig. 7.

CORRESPONDENCE

#### IV. CONCLUSION

Special cases were considered of data fusion of sensors with dissimilar accuracies. It was shown that as the difference in accuracy of the sensors increases, the steady-state solution for track fusion approaches the optimal solution of measurement fusion. In the case of fusion of a cluster of targets resolved by only one of the sensors it was shown that the tracking errors of the fused track may be larger than of the individual sensors. A number of remedies were suggested to this situation involving modifications in the correlation algorithm.

A. M. HAIMOVICH  
Department of Electrical Engineering  
New Jersey Institute of Technology  
Newark, NJ 07102

J. YOSKO  
R. J. GREENBERG  
M. A. PARISI  
JJM Systems, Inc.  
Ivyland, PA 18974  
D. BECKER  
Naval Air Warfare Center  
Warminster, PA 18974

#### REFERENCES

- [1] Blackman, S. S. (1986) *Multiple-Target Tracking with Radar Applications*. Norwood, MA: Artech House, 1986.
- [2] Bar-Shalom, Y., and Fortmann, T. E. (1988) *Tracking and Data Association*. New York: Academic Press, 1988.
- [3] Singer, R. A., and Kanyuck, A. J. (1971) Computer control of multiple site correlation. *Automatica*, 7 (July 1971), 455-463.
- [4] Ditzler, W. R. (1987) A demonstration of multi-sensor tracking. In *Proceedings of the 1987 Tri-Service Data Fusion Symposium*, June 1987, 303-311.
- [5] Bar-Shalom, Y., and Campo, L. (1986) The effect of the common process noise on the two-sensor fused-track covariance. *IEEE Transactions on Aerospace and Electronic Systems*, AES-22 (Nov. 1986), 803-805.
- [6] Roecker, J. A., and McGillem, C. D. (1988) Comparison of two-sensor tracking methods based on state vector fusion and measurement fusion. *IEEE Transactions on Aerospace and Electronic Systems*, 24 (July 1988), 447-449.
- [7] Willner, D., Chang, C. B., and Dunn, K. P. (1976) Kalman filter algorithms for a multi-sensor system. In *Proceedings of the IEEE Conference on Decision and Control*, Dec. 1976, 570-574.
- [8] Chang, C. B., and Younes, L. C. (1982) Measurement correlation for multiple sensor tracking in dense target environment. *IEEE Transactions on Automatic Control*, (Dec. 1982), 1250-1252.
- [9] Barton, D. K. (1976) *Radar System Analysis*. Norwood MA: Artech House, 1976.
- [10] Yosko, J. (1992) Optimal and sub-optimal fusion of  $\alpha - \beta$  target tracks. Masters thesis, Drexel University, Philadelphia, PA, 1992.

- [11] Kalata, P. R. (1984)  
 The tracking index: A generalized parameter for  $\alpha - \beta$   
 and  $\alpha - \beta - \gamma$  target trackers.  
*IEEE Transactions on Aerospace and Electronic Systems*,  
 AES-20 (Mar. 1984), 174-182.

## CW Alternatives to the Coherent Pulse Train—Signals and Processors

We discuss CW signals, phase modulated by a periodic waveform, and their corresponding receivers. The combined response in delay and Doppler is almost identical to the (ideal) response of the coherent pulse train. The receivers are matched to an integral number  $N$  of modulation periods of the transmitted signal. CW implies a duty cycle of 100%. However, the signal duration need not be longer than  $N + 2$  periods. The CW signals have the advantage that their peak power is equal to the average power. Their disadvantage is a more complicated receiver processing and the need for two antennas.

### I. INTRODUCTION

The coherent pulse train (CPT) is one of the most important radar signals. It provides independent control of both delay and Doppler resolution. It also exhibits a range window which is inherently free of sidelobes.

The ambiguity function [1] represents the magnitude of the matched receiver output, in the delay-Doppler domain. The ambiguity function of the CPT indicates that the Doppler resolution is the inverse of the total duration of the signal— $NT$ , while the delay resolution is the pulse duration  $t_p = T/M$ . ( $T$  is the pulse interval,  $N$  is the number of pulses processed coherently, and  $M$  is the inverse of the duty cycle.) The Doppler sidelobes can be reduced by utilizing nonuniform weights (e.g., Hamming) in the receiver. Such a receiver is not matched any more, and the penalties are a signal-to-noise ratio (SNR) loss (1.36 dB for Hamming), and a broadening of the mainlobe in the Doppler dimension. The (central part of the) response of a Hamming weighted receiver to the CPT signal discussed before, is shown in Fig. 1. The figure applies to a CPT signal with  $N = 16$  and  $M = 16$ . In Fig. 1 and all the following three-dimensional (3-D) figures, the delay axis extends over  $-3t_p \leq \tau \leq 2T + 3t_p$ , and the Doppler axis over

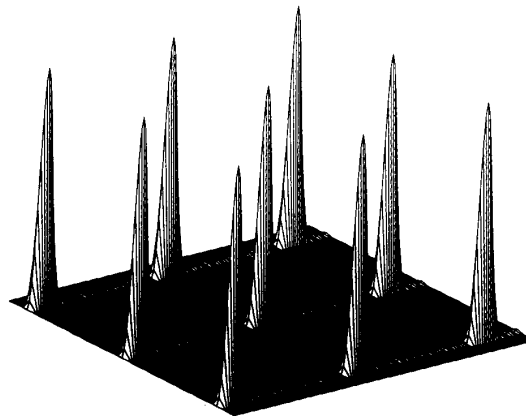


Fig. 1. Delay-Doppler response of Hamming weighted processor to CPT with  $N = 16$  pulses and  $M = T/t_p = 16$ .

$-2/(NT) \leq \nu \leq (2N + 5)/(NT)$ . The vertical axis is linear in voltage units.

Ignoring the unavoidable ambiguity of  $T$  in delay and  $1/T$  in Doppler, the receiver response in Fig. 1 approaches an ideal response. It is this ideal response that makes the CPT such an important radar signal.

The main drawback of the CPT signal is the high ratio of peak to average power. The average power is what determines the detection performances and the estimation accuracy of the parameters of the target. In order to maintain sufficient average power, the CPT signal usually requires high peak power, with all its implications: vacuum tubes, high voltages, heavy transmission lines, etc.

In angle modulated CW signals the peak-to-average power ratio is unit, which allows small solid-state transmitters. On the other hand, CW signals do not readily provide the desired range and Doppler resolution, as depicted in Fig. 1. We show that it is possible to find CW signals and corresponding receivers, whose combined response closely approach the ideal response shown in Fig. 1.

By CW signals we mean periodic signals with 100% duty cycle, i.e., uninterrupted transmission. We do not imply infinitely long signals. As we show later, the receiver processes  $N$  periods of the signal. In order to obtain the desired sidelobe-free response, the received signal has to fill up the processor. This is achieved by a dwell time of  $N + 2$  periods, or longer.

### II. PERIODIC AMBIGUITY FUNCTION

In a recent paper [2] we discussed the Doppler behavior of CW periodic coded sequences, when the receiver processor is matched to an integral number  $N$  of periods of the transmitted signal. We termed the response of such a receiver the "periodic ambiguity function" (PAF), and gave it the symbol  $|\chi_{NT}(\tau, \nu)|$ . ( $\tau$  is delay and  $\nu$  is Doppler frequency shift.) We

Manuscript received June 11, 1991; revised February 8, 1992.

IEEE Log No. T-AES/29/1/02257.

0018-9251/93/\$3.00 © 1993 IEEE